Article

A Novel Salt-Tolerant L-Glutaminase: Efficient Functional Expression, Computer-Aided Design, and Application

Hengwei Zhang, Mengkai Hu, Qing Wang, Fei Liu, Meijuan Xu, Xian Zhang * and Zhiming Rao *

Key Laboratory of Industrial Biotechnology of the Ministry of Education, Laboratory of Applied Microorganisms and Metabolic Engineering, School of Biotechnology, Jiangnan University, Wuxi 214122, China

* Correspondence: zx@jiangnan.edu.cn (X.Z.); raozhm@jiangnan.edu.cn (Z.R.)

Abstract: The low productivity in long fermentation duration and high-salt working conditions limit the application of L-glutaminase in soy sauce brewing. In this study, a novel L-glutaminase (LreuglsA) with eminent salt tolerance was mined and achieved more than 70% activity with 30% NaCl. To improve the robustness of the enzyme at different fermentation strategies, mutation LreuglsA^{H105K} was built by a computer-aided design, and the recombinant protein expression level, an essential parameter in industrial applications, was increased 5.61-fold with the synthetic biology strategy by improving the mRNA stability. Finally, the LreuglsA^{H105K} functional expression box was contributed to *Bacillus subtilis* 168 by auxotrophic complementation, and the production in a 5-L bioreactor was improved to 2516.78 $\pm$ 20.83 U mL^{-1}, the highest production ever reported. When the immobilized cells were applied to high-salt dilute-state soy sauce brewing, the L-glutamate level was increased by 45.9%. This work provides insight into the salt-tolerant enzyme for improving the efficiency of industrial applications.

Keywords: L-glutaminase; computer-aided design; expression level; 5-L bioreactor; high-salt dilute-state soy sauce

1. Introduction

The L-glutamate generated by the reaction is the primary substance responsible for the umami taste of food. Approximately 46% of the L-glutamate in brewed soy sauce is produced from L-glutamine during soy sauce fermentation [1]. Currently, most soy sauces enhance their umami taste by adding monosodium glutamate (MSG), but this often leads to an excessive intake of sodium and thus increases the risk of cardiovascular and cerebrovascular diseases [2,3]. Therefore, the natural enzymatic method can effectively solve this problem by increasing the glutamate content in soy sauce.

L-Glutaminase (EC 3.5.1.2) produces L-glutamate by hydrolyzing the amino group of the amide group in L-glutaminase and is widely distributed in microorganisms such as yeast, bacteria, and fungi [4]. This enzyme has significant potential for application in food and medicine [5]. However, during traditional soy sauce brewing, L-glutaminase activity in *Aspergillus oryzae*, one of the most critical microorganisms in soy sauce Koji, is inhibited because of the high-salt environment, leading to the production of higher levels of the flavorless pyroglutamine rather than the flavor-presenting substance glutamate [6]. Therefore, it is necessary to develop an enzymatic method that can maintain a high stability and enzymatic activity in high-salt soy sauce brewing, which can effectively increase the content of naturally produced L-glutamate in soy sauce products.

According to the current research, the existing L-glutaminase has defects in enzyme activity, stability, and salt tolerance that are not conducive to large-scale industrial production. Kumar et al. found that the L-glutaminase from *Bacillus* sp. LKG-01 (MTCC 10401), isolated from the Gangotri District of Uttarakhand in the Himalayas, is also stable, with 80% relative enzyme activity in the presence of a 25% salt concentration [7]. The

L-glutaminase from *Micrococcus luteus* K-3 showed the maximum enzyme activity in the presence of 1.71 M NaCl, and it showed >90% activity in the presence of 3.08 M NaCl (about an 18% salt concentration) [8,9]. However, the enzyme source is related to food safety, and genetic sources that do not meet the food safety standards are often considered potentially unsafe, and the activity and thermal stability of the enzymes did not meet the industrial requirements. A membrane-bound salt-tolerant and thermally stable L-glutaminase from *Lactobacillus rhamnosus* was screened. The activity of L-glutaminase increased approximately two-fold in the presence of 5% salt, and 90% activity remained in the presence of 15% salt [10]. According to the sodium dodecyl sulfate-polyacrylamide gel electrophoresis (SDS-PAGE) results, one L-glutaminase bound to the cell membrane in *L. reuteri* KCTC3594 was isolated and characterized, and the sizes of the two primary brands of the enzyme were 70 and 50 kDa [11]. Although *L. rhamnosus* and *L. reuteri* are food safe probiotics, the membrane-bound nature of these enzymes increases the complexity of the food brewing process and limits the industrial application of these L-glutaminases (Table 1) [12]. On the other hand, some L-glutaminases also synthesize theanine through glutamyl hydrolysis or the transfer reaction, inhibiting caffeine formation and improving tea broth's flavor [13,14]. In addition to its applications in the food industry, L-glutaminase is used in enzyme therapy for cancer, especially for acute lymphocytic leukemia, because tumor cells have no mechanism to synthesize L-glutamine and take it up as an exogenous resource [15]. The cytotoxic effect of an L-glutaminase from *Bacillus subtilis* OHEM11 (MK389501) indicated significant safety in Vero cells, with high anticancer activity against the NFS-60, HepG-2, and MCF-7 cancer cell lines [16]. L-Glutaminase from *Streptomyces canarius* FR (KC460654) exerted inhibitory effects against Hep-G2 cells, HeLa cells, HCT-116 cells, and RAW 264.7 cells [17].

Table 1. Review of the different sources of glutaminase.

Source	Optimum pH	Optimum Temp (°C)	Specific Gravity (U/mg)	Thermal Stability	Salt Tolerant	References
A. oryzae	9	41	40.12	NR	+	[6]
Bacillus sp. LKG-01	11	70	584.2	+++	+++	[7]
M. luteus K-3	8	50	190	+	+++	[8]
L. rhamnosus	7	50	NR	++	+++	[10]
L. reuteri KCTC3594	7.5	40	16.4	+	++	[11]

NR: No Reported; +: intensity.

Therefore, due to the limitations of a low yield and low enzyme activity of glutaminase, a heterologous high-efficiency expression can solve the problems of high production costs and challenging applications. *B. subtilis*, a Gram-positive model bacterium, has long been used as a microbial cell factory because of its low codon preference, high productivity, and low requirements for fermentation media. In addition, due to its generally regarded as safe (GRAS) status, *B. subtilis* has been used in nutritional food production [18]. Synthetic biology strategies based on *B. subtilis* for enzyme or biochemical production have been developed to render *B. subtilis* more suitable for industrial production [19].

Recently, no publication has reported that a glutaminase can simultaneously possess excellent industrial properties with high enzymatic activity, stability, and salt tolerance. In this study, we mined a nonmembrane-bound L-glutaminase (LreuglsA) from *L. reuteri* DSM20016. LreuglsA had significant specific enzyme activity and exhibited a salt tolerance. Based on a computer-aided rational design, the thermal stability of the enzyme was increased to make it more adaptable for soy sauce production. Subsequently, we replaced the antibiotic resistance gene based on the *B. subtilis*-pMA5 expression system to eliminate the potential hazard to food safety. Moreover, we further increased the expression of LreuglsA in *B. subtilis* by designing a hairpin loop for the ribosome-binding site (RBS) region. Finally, we performed scale-up experiments of the recombinant strain in a 5-L bioreactor and applied the cells in soy sauce brewing after immobilization.

2. Materials and Methods

2.1. Gene Source, Plasmids, and Strains

The host strains for gene cloning and expression were *Escherichia coli* JM109 and *B. subtilis* 168. The shuttle expression plasmid pMA5 was employed for the expression and mutagenesis studies. The DNA fragments containing the L-glutaminase structural gene from *L. reuteri* DSM20016 (NCBI accession number: ABQ83511) were synthesized by GENEWIZ after the codon optimization of *B. subtilis* 168. The C112-02 ClonExpress II One Step Cloning Kit was purchased from Vazyme (Nanjing, China). PCR amplification of the L-glutaminase gene was performed with an appropriate primer pair. Restriction enzymes and PCR reagents were purchased from TaKaRa (Dalian, China). The linearized pMA5 plasmid and glsA genes were assembled to form the recombinant plasmid pMA5-glsA. The TIANprep Mini Plasmid Kit and TIANgel Purification Kit were purchased from Tiangen Biotech (Beijing, China). All experiments were performed according to the product manuals. All other chemicals were purchased from Sinopharm or Merck.

The plasmid was chemically transformed into competent *E. coli* JM109 cells. After extraction and purification from an agarose gel, the plasmid was transformed into *B. subtilis*, and the positive transformants were picked and sent for sequencing to verify the correct sequence. The original strains and plasmids were sourced from our laboratory.

2.2. Bioinformatics Analysis and Screening for Positive Variants

AlphaFold2, an advanced tool for predicting a protein structure based on machine learning, exhibited the best performance in CASP14 [20]. The structural model of LreuglsA was acquired by modeling using AlphaFold2. We validated the multimerization profile of LreuglsA using active page and modeled homologous protein complexes using AlphaFold2-Multimer [21]. The program PyMOL was used to analyze variations in the molecular tertiary structure. The programs Clustal, ESPript 3.0, and Schrödinger Maestro 12.8 were used to determine the active center residues based on multiple sequence alignment (MSA) and ligand docking.

The position-specific scoring matrix (PSSM), representing the conservation of residues, was generated using psiblast in NCBI BLAST 2.9 with uniref90 (https://www.uniprot.org/ (accessed on 3 May 2022)) by setting the number of iterations to 3 and the E-value to 0.01. By analyzing the conservation of these protein residues and evolutionary information from the PSSM, all positions in the protein were examined for the evolvability of the L-glutaminase family and other homologous proteins. The conserved residues were assigned higher scores at the corresponding positions. Based on the PSSM score, we screened evolvable residues to allow mutations. FoldX predicted the overall stability of virtual saturation mutation at all sites and predicted protein thermostability by comparing the changes in Gibbs energy (ddG and $\Delta\Delta G$) after mutation [22]. The conserved residues analyzed from the PSSM were removed from the candidate list. Adverse interactions within the proteins might lead to increased instability of the protein structure. Molecular dynamics (MD) simulations were used to characterize the microscopic evolution of systems at the atomic level by calculating the atomic motion of the protein in the solvent and to visually observe the mechanism and principle of the experimental observation. Based on the calculations obtained from the MD simulation, root mean square fluctuation (RMSF) values further refining the B-factors of the residues were used to indicate the flexible variability at the amino acid sites [23]. In this study, the MD simulation of the qualified models was performed using GROMACS 2019.6 [24].

2.3. Construction of a Food Safe Recombinant B. Subtilis 168 Strain

D-alanine is an essential component of the *B. subtilis* 168 cell wall and is produced by the D-alanine racemase encoded by the alrA gene (Gene ID: 939942). Microorganisms carrying antibiotic resistance genes are usually not allowed in the food industry [25]. The alrA gene was knocked down to obtain a food-grade L-glutaminase-harboring recombinant *B. subtilis* 168 without the antibiotic resistance gene that would be suitable for application

in the food industry. The alrA gene on the replicative plasmids might complement the chromosomal deletion of the alrA gene and provide selective pressure for maintaining the plasmids. The recombinant plasmid pMA5-ΔkanR-alrA-glsA was transformed into *B. subtilis* 168/ΔalrA to obtain strain BSW1.

The alrA gene was knocked out using the Cre/loxP site-specific gene operating system, based on the principle that Cre recombinase specifically recognizes loxP sites and catalyzes the deletion, inversion, and exchange of fragments between two lox sites.

2.4. Overexpression through Synthetic Biology Components

mRNAs play an essential role in posttranscriptional regulation. The secondary structure at the P-terminus of a mRNA is not conducive to ribosome binding and translation initiation. However, some studies have found that a reasonable hairpin structure before the initiation codon ATG will increase, not decrease, the expression of structural genes in eukaryotic cells [26,27]. Viegas and Xiao revealed the feasibility of this strategy in prokaryotic cells of *E. coli* and Bacillus licheniformis, respectively, by assessing the effect of a hairpin structure on the expression [28,29]. In the present study, a hairpin structure was designed directly in front of the open reading frame (ORF), preventing mRNA degradation by the RNA enzyme. The folding free energy of the hairpin rings was calculated using RNAfold [30]. The optimized Shine–Dalgarno (SD) sequence was designed as a single loop after and on the hairpin ring to balance the mRNA–ribosome-binding efficiency and stability. The designed 5'-UTR sequence was inserted in front of the glsA gene by PCR, and pMA5 replaced the original 5'-UTR sequence. Then, chemical transformation was used to construct the *B. subtilis* 168 strain BSW2-BSW9 for overexpression.

For the RT-qPCR analysis of mRNA stability, cells cultured to the logarithmic phase in LB medium were harvested for mRNA extraction. After adding 1 mM rifampicin, the culture was sampled and placed in liquid nitrogen at different times to prevent mRNA degradation. Total RNA was purified using the RNAprep Pure Bacteria Kit (Tiangen Biotech, Beijing, China). The cDNA templates were synthesized with the HiScript II Q RT SuperMix for the qPCR kit (Vazyme Biotech, Nanjing, China) according to the manufacturer's instructions. RT-qPCR was performed using a StepOnePlus instrument (Applied Biosystems, Waltham, MA, USA). The relative expression of the 16S rRNA gene was determined as the internal standard. The primer sequences qPCR-F (ACCAACGACAA-GAAAGCCGA) and qPCR-R (AGACGTTCGATGGCGTACAG) were used for RT-qPCR. The expression levels of LreuglsA were characterized using the 2-ΔΔt method. Each assay was repeated three times.

2.5. L-Glutaminase Expression and Purification

The recombinant strains were cultured in 10 mL of LB medium containing 20 μg mL^{-1} kanamycin for 12 h at 37 °C. Then, a 5% inoculum was transferred to 50 mL of LB medium containing 20 μg mL^{-1} kanamycin, and the cells were cultured for 30 h at 30 °C. The strains were centrifugally separated and washed with phosphate-buffered saline (PBS, pH 7.4). Then, the bacterial suspension was sonicated for 30 min (for 2 s at 5-s intervals) after mixing with 5 mL of PBS containing 20 μL of lysozyme (200 mg/mL). Finally, the mixture was centrifuged at 12,000 rpm for 30 min to separate the cell debris. After centrifugation, the resulting supernatant was a LreuglsA crude enzyme solution and was used to measure the L-glutaminase activity.

A His tag was inserted at the N-terminus of LreuglsA. After SDS-PAGE verification of the expression level, the crude enzyme was purified using Ni-NTA affinity chromatography according to the manufacturer's protocol (GE Healthcare Bio-Sciences, Uppsala, Sweden). The purified LreuglsA and crude enzyme were analyzed using SDS-PAGE analysis.

2.6. Enzyme Activity Assay

The L-glutaminase activity was calculated by testing the L-glutamate content produced. The reaction was performed at a specific temperature for 5 min and terminated by

adding 100 μL of 15% trichloroacetic acid (TCA). The reaction mixture (1 mL) contained 880 μL of 200 mM L-glutamine and 20 μL of L-glutaminase. After centrifugation, the L-glutamate concentration in the supernatant was measured using a biosensor analyzer (Institute of Biology, Shandong Academy of Sciences). One unit (U) of enzymatic activity of L-glutaminase was defined as the amount of enzyme required to produce 1 μmol of L-glutamate per minute. The Bradford Protein Assay Kit (Sangon Biotech (Shanghai) Co., Ltd., Shanghai, China) was used to determine the protein concentration according to the manufacturer's instructions.

### 2.7. Fermentation and Application of L-Glutaminase in Soy Sauce Brewing

The production capacity of the bioreactor shows the industrial application potential of the recombinant strain. The recombinant bacterial strain was cultured by two-stage seed expansion, and 100 mL of the seed culture were transferred into a 5-L bioreactor (Dibi'er Bio-Engineering Co., Ltd., Shanghai, China) containing 2 L of fermentation medium. DO-stat fed-batch fermentation strategies were used for fermentation. The pH was maintained at 7.0 using NH_4OH (30% *v/v*) and the feed medium (sucrose, 500 g L^{-1}; K_2HPO_4, 2.612 g L^{-1}; KH_2PO_4, 2.041 g L^{-1}; $MgSO_4 \cdot 7H_2O$, 1.845 g L^{-1}; and NaCl, 5 g L^{-1}).

Studies have shown that brewed soy sauce is rich in nutrients and contains a variety of physiologically active substances. High-salt diluted-state (HSDS)-brewed soy sauce has a rich and full-bodied aroma and taste [6]. The soybeans were cleaned and separated, soaked for 8 h, and then steamed at 125 °C for 15 min. The cooked soybeans were naturally cooled to 40 °C and then mixed (soybean:flour = 4:1, 0.05% spores of a species) to obtain a 0-h sample of Koji, which was then placed in an incubator for culture. Then, the soybeans were placed in the incubator to produce the Koji. The Koji was turned in a timely manner during the incubation process to control the temperature of the product, and the temperature was not allowed to exceed 28–30 °C to prevent burning. After 44 h, the finished product was obtained. The mash was mixed with brine (24° Be/20 °C) at a ratio of 1:2.2 and placed in an incubator at 37 °C for fermentation. After 120 days, the soy sauce was sampled and filtered to obtain raw soy sauce and, finally, heat-treated at 90 °C for 30 min to obtain sterilized soy sauce. The free amino acid content in the finished soy sauce was determined using HPLC.

3. Results and Discussion

3.1. A Novel L-Glutaminase Displays Significant Salt Tolerance

As a GRAS strain, the application value of *B. subtilis* in the food industry is self-evident [19]. A food safe strain without antibiotic resistance must be constructed. The Food and Agriculture Organization of the United Nations (FAO) and the World Health Organization (WHO) have stressed that antibiotic resistance genes that are resistant to clinically used antibiotics should not appear in food [31]. The food-grade strain BSW1 lacking the alrA gene and transformed with pMA5-ΔkanR-alrA-glsA was successfully constructed to obtain the recombinant L-glutaminase-expressing strain for food industry applications (Figure 1A). After 30 h of cultivation in LB medium, the intracellular L-glutaminase activity was 16.32 ± 0.56 U mL^{-1}, and the expression of LreuglsA was analyzed using SDS-PAGE (Figure 1B). A 6His tag was added to the N-terminus of LreuglsA, and Ni^{2+} affinity chromatography was used to purify LreuglsA. Separation on a 12% SDS-PAGE gel indicated that the protein was purified and that the molecular mass was approximately 30 kDa, as previously predicted (Figure 1C).
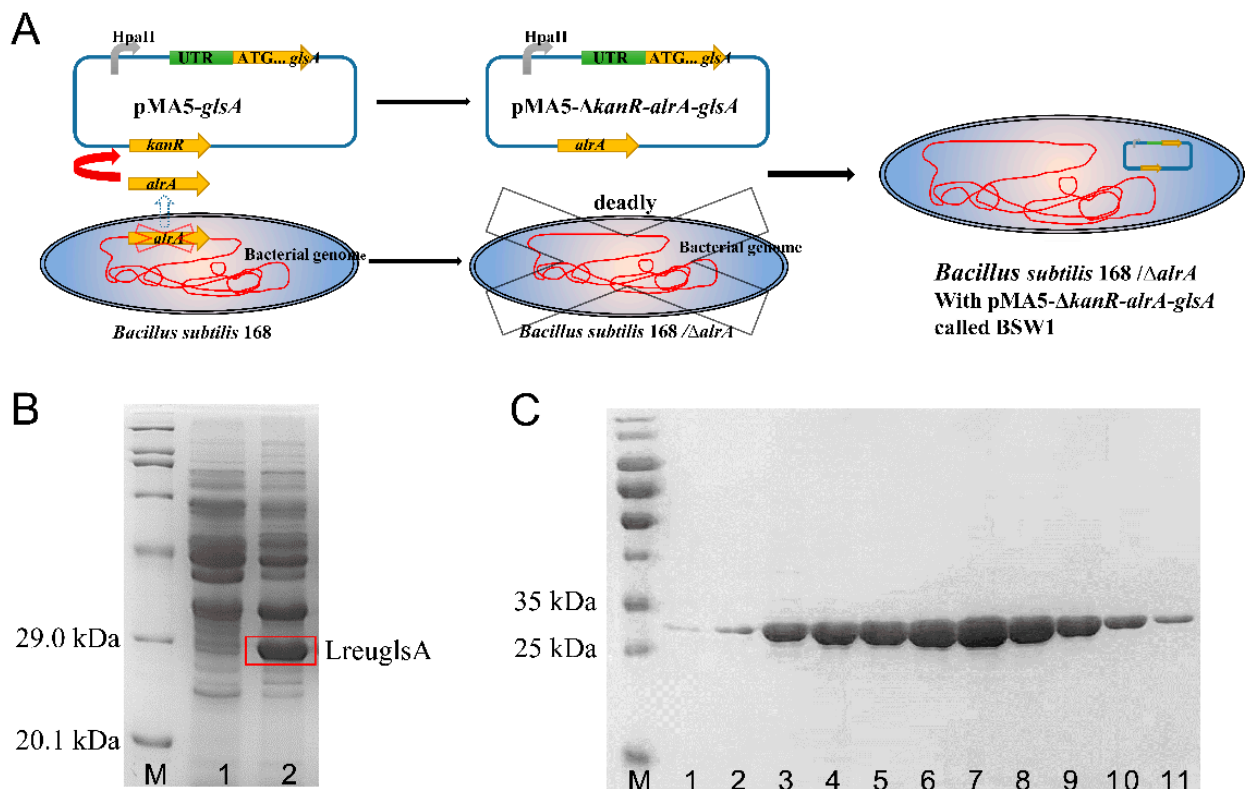
Figure 1. Construction of food-grade *B. subtilis*. (**A**) *B. subtilis* 168, in which the *alrA* gene was knocked down, did not grow in basic medium. D-Alanine was added when screening the auxotrophic strain *B. subtilis* 168/Δ*alrA*. The recombinant plasmid pMA5-ΔkanR-*alrA*-glsA, in which the alrA gene was used to replace the pMA5 recombinant plasmid containing the Kan resistance gene, was transformed into *B. subtilis* 168/ΔalrA. (**B**) SDS-PAGE analysis of LreuglsA expression in BSW1. The three lanes show the marker (Lane M), pMA5-ΔkanR-alrA expression in BSW0 (Lane 1), and pMA5-ΔkanR-*alrA*-glsA expression in BSW0 (Lane 2). The protein size was approximately 30 kDa, according to the marker. (**C**) SDS-PAGE analysis of purified LreuglsA. Ni2+-affinity chromatography was used to purify the protein. The gradient elution process of protein samples during purification is reflected in the image (Lanes 1–11).

The enzymatic properties play a decisive role in the industrial application of enzyme preparations. The enzymatic reaction was performed under different conditions to investigate the properties of LreuglsA. The maximum reaction rate was achieved at a temperature of 50 °C and pH 7.5 (50 mM Tris-HCl buffer, Figure 2A,B). The specific activity of the purified enzyme was 1048.14 ± 7.83 U mg^{-1}. The enzyme remained stable (more than 60% activity remained) after an incubation for 216 h at 4 °C in pH 6–7 buffer without any protective agent. In terms of temperature stability, the enzyme reached a T1/2 of approximately 44 h at an industrial working temperature of 37 °C; however, the activity reduced to less than 50% after 30 min of incubation at 50 °C (Figure 2C). The enzyme kinetic constant Km was measured as 51.24 ± 4.39 mM, and the Vmax was 7.84 ± 0.33 mM min^{-1} under the optimum reaction conditions (Figure 2D). We investigated the effect of adding 1 mM metal ions on the enzyme activity. Na$^+$ activated the enzyme, and the other metal ions inhibited (less than 30%) the enzyme to some extent (Figure 2E).
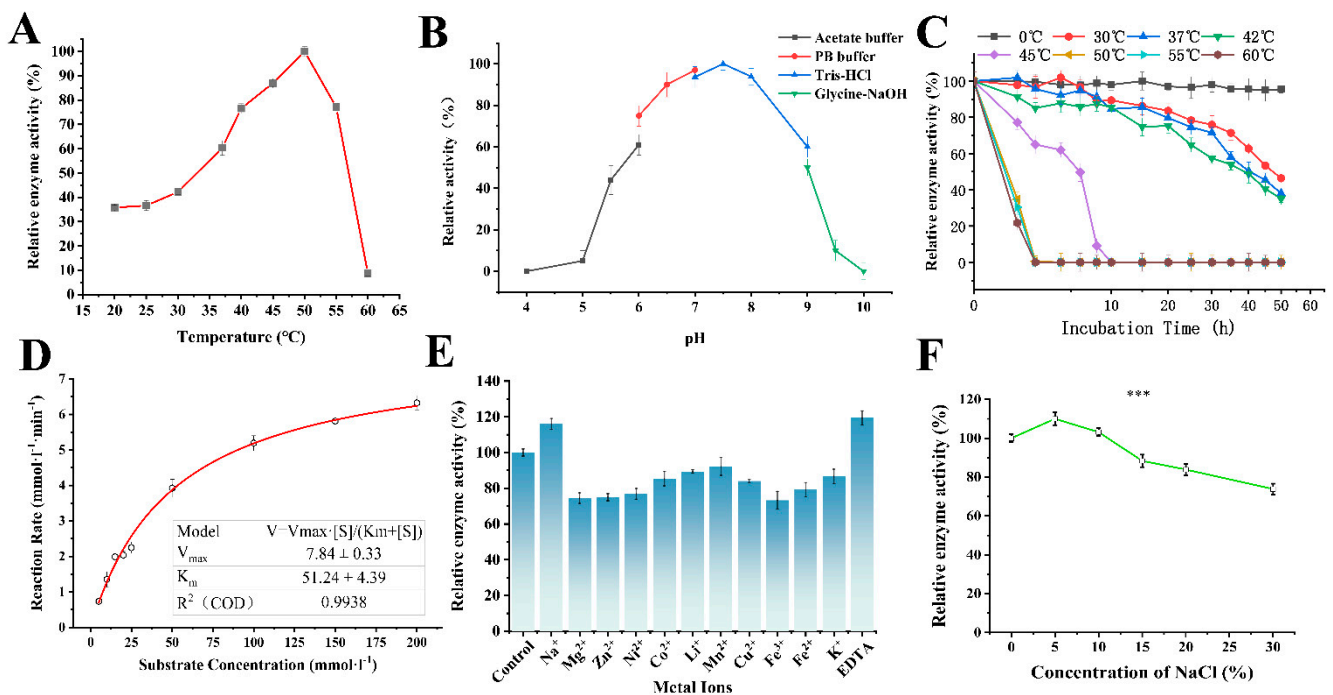
Figure 2. Enzymatic properties of LreuglsA. The activities are presented as relative values observed in various ranges, as described below. (**A**) Effect of temperature on LreuglsA activity. (**B**) Effect of pH on LreuglsA activity. (**C**) Effect of stability at different temperatures on LreuglsA activity. (**D**) Enzyme kinetic fitting. The Michaelis–Menten equation was applied using the Origin nonlinear fitted Hill function ($n = 1$). (**E**) Effect of metal ions on LreuglsA activity. (**F**) Effects of salt concentrations on the glutaminase activity of LreuglsA. Each experimental data point represents the average of three independent experiments, and the error bars indicate standard deviations. *** $p < 0.005$.

The most significant feature for the industrial value of LreuglsA was its salt tolerance. The high-salt normothermic conditions in brewing processes such as those of soy sauce limit the application of food enzyme preparations. The LreuglsA enzyme activity peaked at a 5% salt concentration, reaching 110.03% of the activity measured under blank conditions. At a near-saturated NaCl concentration (30%), 73.85% of the activity under blank conditions was maintained (Figure 2F). Moreover, in 20% NaCl solution, the thermal stability of the enzyme increased by more than 70% at 50 °C. A potential explanation for this result may be that, at low salt concentrations, the ions in the solvent enhance the interaction force of hydrophobic residues inside the protein and increase the stability. However, at high salt concentrations, the weakening of the hydrated layer formed by the charged residues on the protein surface and the increasing difficulty of the active pocket to take up substrates from the solvent lead to a decrease in enzyme activity. Based on these data, LreuglsA has a good potential for industrialization. Its ability to maintain the necessary activity under high-salt conditions indicates that it can be used in high-salt industrial brewing processes such as those used for soy sauce.
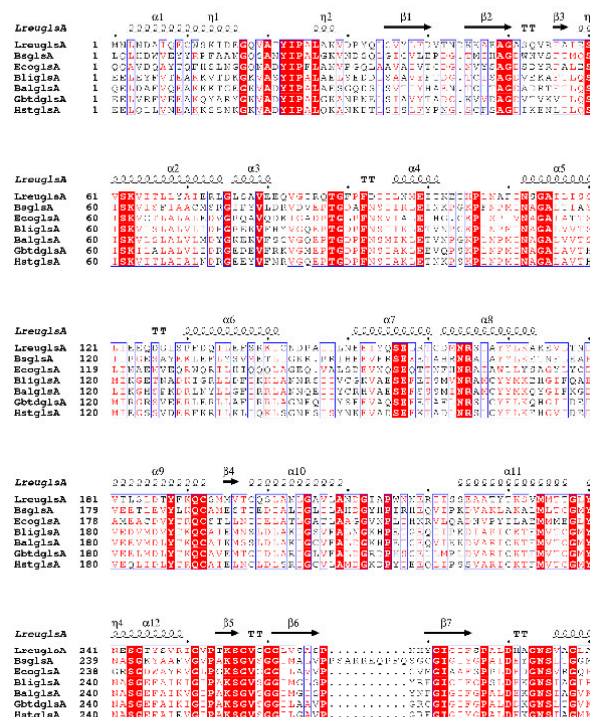
3.2. Structural Prediction and Identification of the Active Center of LreuglsA

AlphaFold2 is a valuable tool to obtain deeper insights into the structure of the LreuglsA protein. The active page shows a comparable molecular weight of active LreuglsA to the bovine serum protein (66.43 kDa), suggesting that, in the reactivated state, LreuglsA is present in a homodimeric form. We obtained a dimer model with an "iptm + ptm" score of 0.93 and a residue pLDDT score greater than 80 using AlphaFold2-Multimer for homologous dimer modeling.

Thus far, we have identified the possible active sites by performing a sequence alignment between LreuglsA and glutaminases from *Bacillus amyloliquefaciens* (BalglsA),

B. subtilis (BsglsA), *B. licheniformis* (BliglsA), *E. coli* (EcoglsA), *Geobacillus stearothermophilus* (GbtglsA), and *Heyndrickxia sporothermodurans* (HstglsA) to identify possible LreuglsA active sites ([32] Figure 3A), combined with the structural analysis of BsglsA and EcoglsA and alignment of highly conserved sequences. In the catalytic pocket, we identified a catalytic triplet, S60-V61-S62-K63, which is the β-lactamase motif (S-X-X-K) and is considered essential for catalysis [33]. We screened a suitable docking result using Glide version 91117 (mmshare version 54117) in Maestro 12.8 software for molecular docking, with the following docking values: Best Emodel = −42.29, E = −34.31, Eint = 7.15, and GlideScore = −4.56. The amino acid residues E59, S60, E157, and Y188 form hydrogen bonds with L-glutamine (Figure 3B). Based on Schrödinger Glide Docking, we mutated the residues into alanine to verify the reliability of the molecular docking results. After mutating each of the four residues mentioned above that form hydrogen bonds with glutamine, the glutaminase was inactive. These results allowed us to determine the active center of LreuglsA.
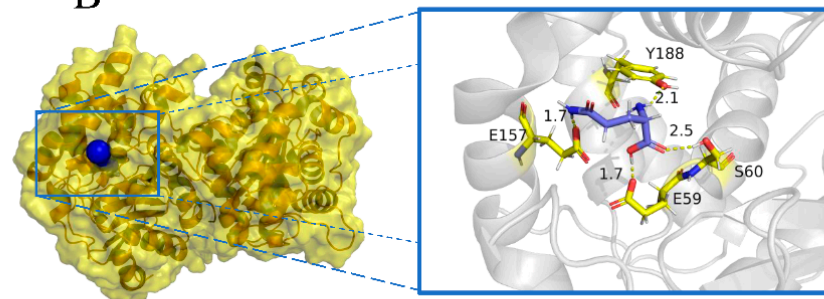

Figure 3. Structural prediction and identification of the active center. (**A**) Analysis of conserved residues required for enzyme function by a sequence alignment of known L-glutaminases. The color scheme option was normal in ESPript 3 (http://espript.ibcp.fr (accessed on 3 May 2022)). (**B**) The PDB structure generated by AlphaFold2-Multimer and molecular docking via Schrödinger. The images were generated using PyMOL. The blue part is the substrate entry and exit channel.

3.3. A H105K Mutant Is Designed Using Computer-Aided Mutation Prediction to Increase Thermostability

In industrial applications, temperature stability has always been an issue of concern. Greater temperature stability may broaden the prospective applications of LreuglsA. We identified regions of LreuglsA with high RMSF values by performing an MD simulation and screened for energy differences using FoldX for virtual saturation mutations in the entire sequence to increase the temperature stability. Mutations in residues near the active pocket were excluded, as these residues may be critical for the reaction (Figure 4A). Meanwhile, evolutionary information was employed by PSSM to identify positions that might be mutated into conserved residues related to heat resistance in L-glutaminase (Figure 4B). Based on the computer-aided mutation prediction, eight mutant sites were selected after a visual inspection, and the mutants were expressed in *B. subtilis* 168.
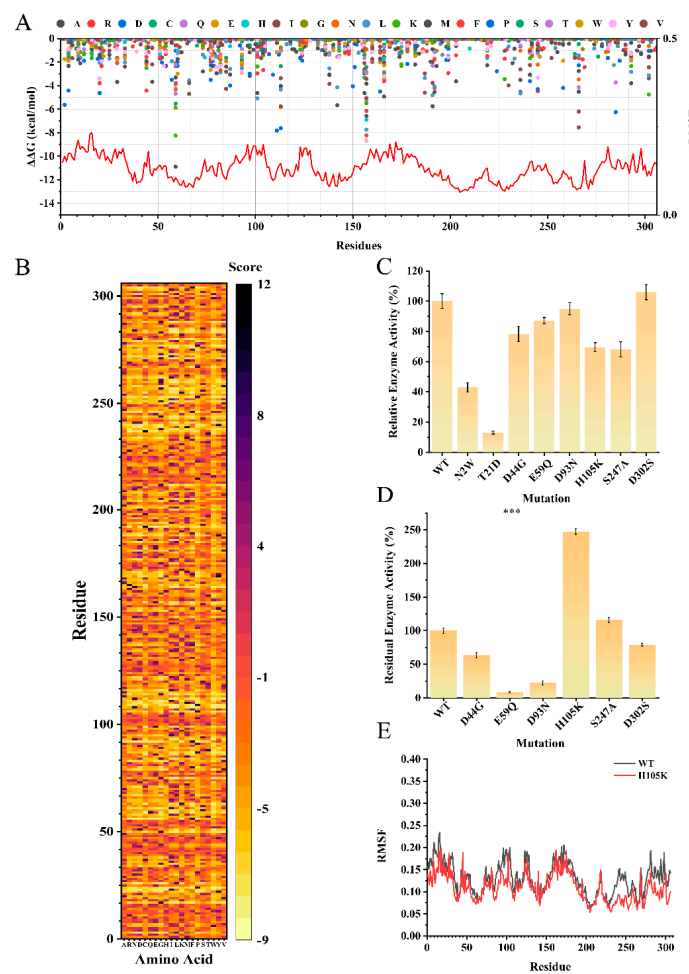

Figure 4. Computer-aided mutation prediction for increasing the thermostability. (**A**) The ddG value of the virtual saturation mutation and the RMSF of LreuglsA. The colored circles represent the energy change after virtual mutation, and the part where ddG is positive is not shown. The red line is the RMSF of LreuglsA, which indicates the side-chain flexibility of LreuglsA. (**B**) Evolvable residues based on the PSSM score to allow mutations. The more conserved amino acids scored higher at this position. (**C**) Enzyme activity of mutants reacted at 50 °C for 5 min. The activities are presented as relative values observed for the mutants. (**D**) Enzyme activity of mutants after 72 h of incubation at 37 °C. *** $p < 0.005$. (**E**) RMSF values of the side-chain atoms for the WT and H105K systems. The black line represents the outcome for the WT system, and the red line represents the outcome for the H105K system. The activities are presented as relative values observed for the mutants. Each experimental data point is the average of three independent experiments, and the error bars indicate standard deviations.

As the solvent environment of crude enzymes is closer to that of industrial catalytic microbial cell factories, crude enzymes are used to screen mutants with improved stability, and according to the report, the change of the folding free energy of different mutants will affect the protein expression level. The thermodynamic stabilities of the wild-type and mutant enzymes were compared at 37 °C. Crude enzyme activity was determined at 50 °C to exclude variants with decreased activity compared to wild-type LreuglsA (Figure 4C). After an incubation at 37 °C for 72 h, the residual enzyme activity of L-glutaminase was measured to compare the thermostabilities of the wild-type and mutant proteins. The results of the preliminary screen suggested that the enzyme activity of the N2W and T21D mutants was 50% lower than that of the wild-type enzyme (Figure 4C). No follow-up studies were conducted for these two mutation sites. After 72 h of incubation, the relative enzyme activity of the H105K mutant was 247.36% of that of the wild-type enzyme. A comparison of the RMSF values of the H105K mutant and the wild-type enzyme by MD simulations of 30 ns at 37 °C showed that the H105K mutant was less structurally flexible than the wild-type protein, resulting in the excellent thermal stability of the H105K mutant (Figure 4D). Additionally, an energy-based ddG of -1.93 kJ mol^{-1} confirmed this possibility. Next, we verified the salt tolerance of the H105K mutant, and the relative enzyme activity in the presence of 20% NaCl reached more than 85% of that measured in the absence of NaCl, indicating that the mutation did not affect the salt tolerance of LreuglsA.

3.4. Improving Enzyme Production with a Portable 5′-UTR

The secondary hairpin structure of the 5′-UTR has been reported to increase the stability of mRNA, thereby increasing the level of structural gene expression. A series of particular secondary structures based on the RBS of pMA5 were developed and inserted into the 5′-UTR as a stabilizer to increase the translation efficiency (Figure 5A). The sequence of the 5′-UTR used in this study is listed in Figure 5A. We included the completely unpaired SD sequence within or after the hairpin loop to adjust the distance between the hairpin structure and ATG. Driven by BSW3 (with UTR3), the L-glutaminase activity increased 5.61-fold from 16.32 ± 0.56 U mL^{-1} to 91.56 ± 2.43 U mL^{-1} (Figure 5B). The bound ribosome and hairpin ring secondary structure protected the mRNA from digestion, as described in previous research. RT-qPCR was performed to determine the stability of the mRNA after the addition of the UTR element. The RT-qPCR results showed that the half-life of the mRNA containing UTR3 was 5.2-fold higher than that of the control group (Figure 5C). Thus, in *B. subtilis*, synthetic biological 5′-UTR components represent a new strategy to increase the protein expression. As shown by the RNAfold results, the original RBS region of pMA5 also formed a hairpin loop structure. However, the SD sequence was present in paired bases, which was unfavorable for ribosome recognition and binding.

In contrast, for the artificially designed RBS sequence, the SD sequence located in the loop did not affect ribosome binding. However, the effect of different minimum free energies of hairpin loops on the expression was noticeable. The finer optimization of the minimum free energy for hairpin ring uncoupling warrants further investigation.
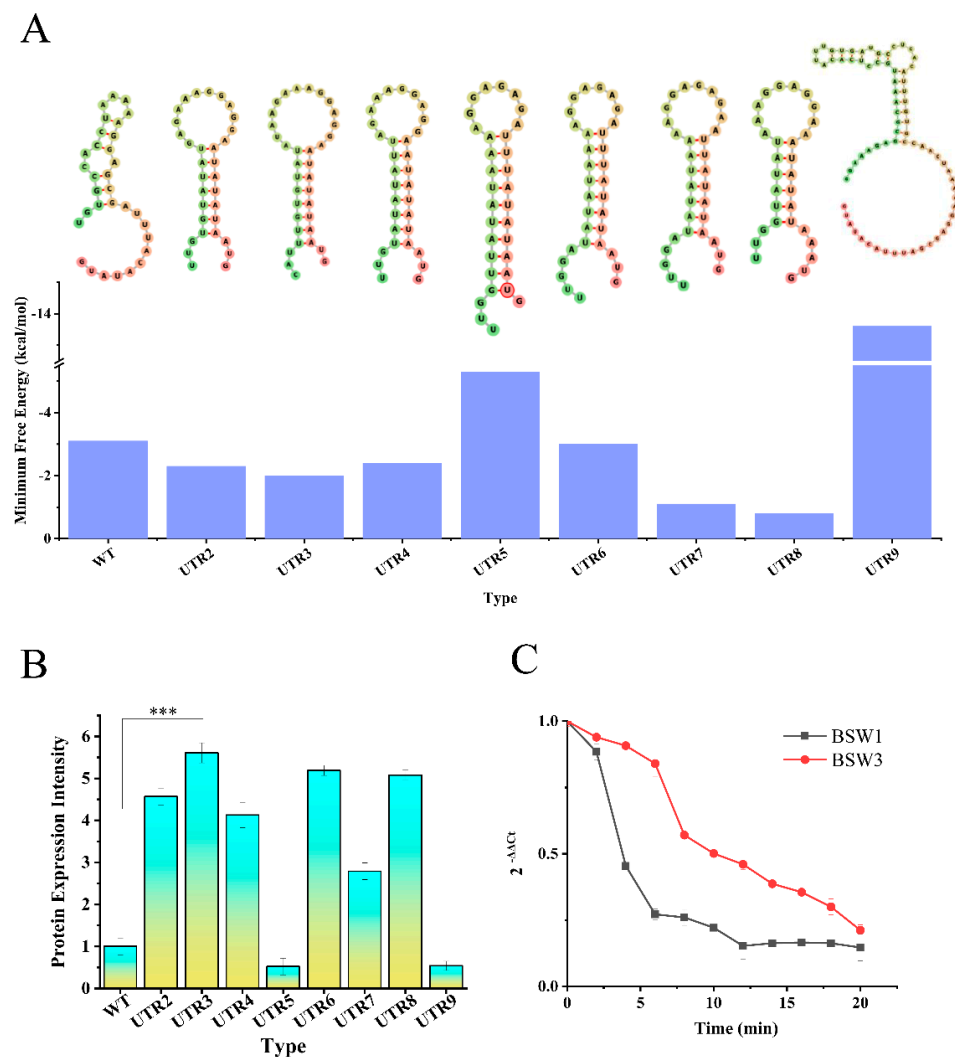
Figure 5. Protein overexpression with a portable 5′-UTR. (**A**) MFE plain structures of the 5′-UTR and its corresponding minimum free energy values are presented in the bar chart below. (**B**) Protein expression levels from constructs with different 5′-UTRs located before the ATG start codon. *** $p < 0.005$. (**C**) Intracellular LreuglsA mRNA levels in BSW1 and BSW3 at different times after the addition of rifampicin. Each experimental data point is the average of three independent experiments, and the error bars indicate standard deviations.

3.5. Immobilized BSW3-H105K Cells Significantly Increase Glutamate Production during Soy Sauce Brewing

Generally, because stirred-tank bioreactors have a more automated control system, they provide a better production environment for microbial cell factories. Therefore, the process for the production of LreuglsA by BSW3 was transferred to a 5-L bioreactor to evaluate the kinetic parameters during scale-up. We selected the most suitable fermentation medium for LreuglsA by BSW3-H105K cells using speed–DO-coupled replenishment (Figure 6A). During fermentation, with DO controlled at 35% and the stirring rate down-off, feeding was started at 15 mL/h when the DO content was higher than 40% in the logarithmic growth phase of fermentation, and the feed flow rate was increased when the DO content started increasing again. Eventually, the L-glutaminase activity reached 2516.78 ± 20.83 U mL^{-1}, and the OD600 reached 93.90 ± 2.01. Regarding enzyme production, by exploring the bacterial growth curve and enzyme production kinetics, L-glutaminase was identified as a growth-associated product in the bioreactor culture, with an average yield of 26.79 U mL^{-1} per unit OD600 (Figure 6B).
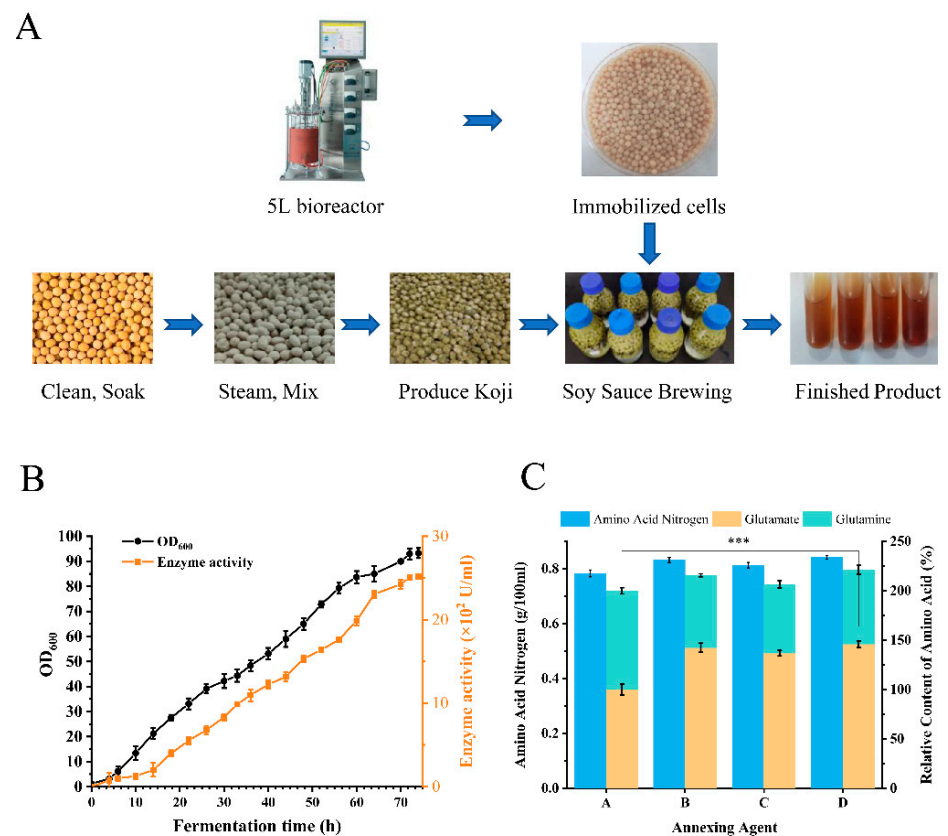
Figure 6. Fermentation, immobilization, and soy sauce brewing. (**A**) BSW3 was fermented in a 5-L bioreactor, and 500 mL of cells were immobilized after fermentation; the resulting immobilized cells were added to the HSDS soy sauce brew in six portions. (**B**) The fermentation process parameters of the recombinant strain BSW3 in 5-L fed-batch fermentation. (**C**) Levels of amino acid nitrogen, glutamate, and glutamine in the produced soy sauce. Group A was the control group, the cell-disrupting crude enzyme was added to group B, washed whole cells were added to group C, and immobilized cells were added to group D. Each experimental data point represents the average of three independent experiments, and the error bars indicate standard deviations. *** $p < 0.005$.

The addition of LreuglsA to the soy sauce brewing process revealed the potential applicability of this enzyme in the brewing industry. The levels of amino acid nitrogen and free amino acids are the characteristic indexes used to determine the degree of fermentation in soy sauce brewing. Cell immobilization can effectively prolong the stability of the enzyme [34], and the addition of immobilized cells in the soy sauce brewing process might effectively prevent the cell contents and the enzyme itself from influencing the flavor of the soy sauce (Figure 6A). Cells harvested from 500 mL of fermentation culture were washed with PBS and mixed with an equal volume of 2.5% sodium alginate. The mixture was dropped through a syringe into a 10% $CaCl_2$ solution to form immobilized capsules of 3–5 mm. In soy sauce brewing, crude enzyme liquid, whole cells, and immobilized cells (prepared separately from the same batch of 500 mL of fermentation broth) were divided into six batches and added to the fermentation solution every 20 days. The formaldehyde method was used to determine the amino acid nitrogen content, and HPLC was used to determine the free amino acid content. According to the Chinese hygiene standards for soy sauce (GB/T 18186-2000), the soy sauce from the control group without additives reached the first-class standard with a 0.783 ± 0.003 g per 100 mL amino acid nitrogen content, and soy sauce fermented with immobilized BSW3 reached the superfine standard with a final amino acid nitrogen content of 0.841 ± 0.002 g per 100 mL. Regarding the glutamate content, the addition of all three forms of glutaminase increased the glutamate content, with the best-immobilized BSW3 increasing it by 45.9% from 5.0152 ± 0.048 g L^{-1}

to 7.319 ± 0.068 g L^{-1} (Figure 6C). Thus, the addition of salt-tolerant LreuglsA to the soy sauce brewing process increased the L-glutamate content in the soy sauce and improved its quality. Laboratory-level soy sauce brewing may reveal the potential of this strategy for soy sauce production. The application of immobilized cells in soy sauce potentially improves the enzyme stability and multibatch utilization and effectively reduces the alteration of soy sauce flavor due to the presence of food additives. Although cell immobilization may provide more favorable working conditions for the enzyme, high-salt conditions are not conducive to the maintenance of the stability of recombinant bacteria. These results will be valuable for investigating the directed evolution of salt tolerance of host bacteria and the immobilization of enzymes.

4. Conclusions

In this work, a food-grade recombinant bacterium was constructed with a salt-tolerant L-glutaminase based on a synthetic biology strategy. First, we mined for a novel L-glutaminase with significant salt tolerance and enzymatic activity, and based on AlphaFold2 modeling and computational biology, we screened for mutation sites with enhanced temperature stability. By optimizing the free energy of the 5′-UTR and synthetic biological application of the *alrA* gene, the constructed food-grade BSW3 achieved an enzyme activity of 2516.78 ± 20.83 U/mL in a 5-L bioreactor, which is the highest production reported to date. Finally, the immobilized BSW3 was effective in soy sauce brewing, improving the glutamic acid, the important flavoring substance in soy sauce, by 45.9%. This study provided reference for further improving the quality of soy sauce, and the study of salt tolerance of the enzyme provided valuable material.

Author Contributions: Conceptualization, Z.R. and X.Z.; methodology, H.Z., F.L., M.X. and M.H.; software, H.Z.; validation, H.Z.; formal analysis, M.X.; investigation, M.H. and Q.W.; resources, M.H.; data curation, H.Z.; writing—original draft preparation, H.Z.; writing—review and editing, H.Z.; visualization, M.H.; supervision, H.Z.; project administration, Z.R. and X.Z.; and funding acquisition, Z.R. and X.Z. All authors have read and agreed to the published version of the manuscript.

Institutional Review Board Statement: Not applicable.

Informed Consent Statement: Not applicable.

Data Availability Statement: The data that support the findings of this study are available from the corresponding author upon reasonable request.

Conflicts of Interest: The authors declare no conflict of interest.

References

1. Halpern, B.P. Glutamate and the flavor of foods. *J. Nutr.* **2000**, *130*, 910S–914S. [CrossRef] [PubMed]
2. Geha, R.S.; Beiser, A.; Ren, C.; Patterson, R.; Greenberger, P.A.; Grammer, L.C.; Ditto, A.M.; Harris, K.E.; Shaughnessy, M.A.; Yarnold, P.R.; et al. Review of alleged reaction to monosodium glutamate and outcome of a multicenter double-blind placebo-controlled study. *J. Nutr.* **2000**, *130*, 1058S–1062S. [CrossRef] [PubMed]
3. Graudal, N.A.; Hubeck-Graudal, T.; Jurgens, G. Effects of low sodium diet versus high sodium diet on blood pressure, renin, aldosterone, catecholamines, cholesterol, and triglyceride. *Cochrane Database Syst. Rev.* **2020**, *12*, CD004022. [CrossRef] [PubMed]
4. Binod, P.; Sindhu, R.; Madhavan, A.; Abraham, A.; Mathew, A.K.; Beevi, U.S.; Sukumaran, R.K.; Singh, S.P.; Pandey, A. Recent developments in l-glutaminase production and applications—An overview. *Bioresour. Technol.* **2017**, *245*, 1766–1774. [CrossRef]
5. Nandakumar, R.; Yoshimune, K.; Wakayama, M.; Moriguchi, M. Microbial glutaminase: Biochemistry, molecular approaches and applications in the food industry. *J. Mol. Catal. B Enzym.* **2003**, *23*, 87–100. [CrossRef]
6. Tadanobu Nakadai, S.N. Use of Glutaminase for Soy Sauce Made by Koji or a Preparation of Proteases from Aspergillus oryzae. *J. Ferment. Bioeng.* **1989**, *67*, 158–162. [CrossRef]

7. Kumar, L.; Singh, B.; Adhikari, D.K.; Mukherjee, J.; Ghosh, D. A temperature and salt-tolerant L-glutaminase from gangotri region of uttarakhand himalaya: Enzyme purification and characterization. *Appl. Biochem. Biotechnol.* **2012**, *166*, 1723–1735. [CrossRef]
8. Nandakumar, R.; Wakayama, M.; Nagano, Y.; Kawamura, T.; Sakai, K.; Moriguchi, M. Overexpression of salt-tolerant glutaminase from Micrococcus luteus K-3 in Escherichia coli and its purification. *Protein Expr. Purif.* **1999**, *15*, 155–161. [CrossRef]
9. Moriguchi, M.; Sakai, K.; Tateyama, R.; Furuta, Y.; Wakayama, M. Isolation and Characterization of Salt-Tolerant Glutaminases from Marine Micrococcus-Luteus K-3. *J. Ferment. Bioeng.* **1994**, *77*, 621–625. [CrossRef]
10. Weingand-Ziade, A.; Gerber-Decombaz, C.; Affolter, M. Functional characterization of a salt- and thermotolerant glutaminase from Lactobacillus rhamnosus. *Enzym. Microb. Technol.* **2003**, *32*, 862–867. [CrossRef]
11. Jeon, J.M.; Lee, H.I.; Han, S.H.; Chang, C.S.; So, J.S. Partial purification and characterization of glutaminase from Lactobacillus reuteri KCTC3594. *Appl. Biochem. Biotechnol.* **2010**, *162*, 146–154. [CrossRef]
12. Amobonye, A.; Singh, S.; Pillai, S. Recent advances in microbial glutaminase production and applications-a concise review. *Crit. Rev. Biotechnol.* **2019**, *39*, 944–963. [CrossRef] [PubMed]
13. Pu, H.; Wang, Q.; Zhu, F.; Cao, X.; Xin, Y.; Luo, L.; Yin, Z. Cloning, expression of glutaminase fromPseudomonas nitroreducensand application to theanine synthesis. *Biocatal. Biotransform.* **2012**, *31*, 1–7. [CrossRef]
14. Sakhaei, M.; Alemzadeh, I. Enzymatic Synthesis of Theanine in the Presence of L-glutaminase Produced by Trichoderma koningii. *Appl. Food Biotechnol.* **2017**, *4*, 113–121. [CrossRef]
15. Kroemer, G.; Pouyssegur, J. Tumor cell metabolism: Cancer's Achilles' heel. *Cancer Cell* **2008**, *13*, 472–482. [CrossRef] [PubMed]
16. Orabi, H.; El-Fakharany, E.; Abdelkhalek, E.; Sidkey, N. Production, optimization, purification, characterization, and anti-cancer application of extracellular L-glutaminase produced from the marine bacterial isolate. *Prep. Biochem. Biotechnol.* **2020**, *50*, 408–418. [CrossRef]
17. Reda, F.M. Kinetic properties of Streptomyces canarius L- Glutaminase and its anticancer efficiency. *Braz. J. Microbiol.* **2015**, *46*, 957–968. [CrossRef]
18. Liu, Y.; Su, A.; Li, J.; Ledesma-Amaro, R.; Xu, P.; Du, G.; Liu, L. Towards next-generation model microorganism chassis for biomanufacturing. *Appl. Microbiol. Biotechnol.* **2020**, *104*, 9095–9108. [CrossRef]
19. Liu, Y.; Liu, L.; Li, J.; Du, G.; Chen, J. Synthetic Biology Toolbox and Chassis Development in Bacillus subtilis. *Trends Biotechnol.* **2019**, *37*, 548–562. [CrossRef]
20. Jumper, J.; Evans, R.; Pritzel, A.; Green, T.; Figurnov, M.; Ronneberger, O.; Tunyasuvunakool, K.; Bates, R.; Zidek, A.; Potapenko, A.; et al. Highly accurate protein structure prediction with AlphaFold. *Nature* **2021**, *596*, 583–589. [CrossRef]
21. Evans, R.; O'Neill, M.; Pritzel, A.; Antropova, N.; Senior, A.; Green, T.; Žídek, A.; Bates, R.; Blackwell, S.; Yim, J.; et al. Protein complex prediction with AlphaFold-Multimer. *BioRxiv* **2022**. [CrossRef]
22. Schymkowitz, J.; Borg, J.; Stricher, F.; Nys, R.; Rousseau, F.; Serrano, L. The FoldX web server: An online force field. *Nucleic Acids Res.* **2005**, *33*, W382–W388. [CrossRef] [PubMed]
23. Sun, Z.; Liu, Q.; Qu, G.; Feng, Y.; Reetz, M.T. Utility of B-Factors in Protein Science: Interpreting Rigidity, Flexibility, and Internal Motion and Engineering Thermostability. *Chem. Rev.* **2019**, *119*, 1626–1665. [CrossRef] [PubMed]
24. Abraham, M.J.; Murtola, T.; Schulz, R.; Páll, S.; Smith, J.C.; Hess, B.; Lindahl, E. GROMACS: High performance molecular simulations through multi-level parallelism from laptops to supercomputers. *SoftwareX* **2015**, *1–2*, 19–25. [CrossRef]
25. Xia, Y.; Chen, W.; Zhao, J.X.; Tian, F.W.; Zhang, H.; Ding, X.L. Construction of a new food-grade expression system for *Bacillus subtilis* based on theta replication plasmids and auxotrophic complementation. *Appl. Microbiol. Biotechnol.* **2007**, *76*, 643–650. [CrossRef]
26. Schwanhausser, B.; Busse, D.; Li, N.; Dittmar, G.; Schuchhardt, J.; Wolf, J.; Chen, W.; Selbach, M. Global quantification of mammalian gene expression control. *Nature* **2011**, *473*, 337–342, Erratum in *Nature* **2013**, *495*, 126–127. [CrossRef]
27. Kozak, M. Influences of mRNA secondary structure on initiation by eukaryotic ribosomes. *Proc. Natl. Acad. Sci. USA* **1986**, *83*, 2850–2854. [CrossRef]
28. Viegas, S.C.; Apura, P.; Martinez-Garcia, E.; de Lorenzo, V.; Arraiano, C.M. Modulating Heterologous Gene Expression with Portable mRNA-Stabilizing 5′-UTR Sequences. *ACS Synth. Biol.* **2018**, *7*, 2177–2188. [CrossRef]
29. Xiao, J.; Peng, B.; Su, Z.; Liu, A.; Hu, Y.; Nomura, C.T.; Chen, S.; Wang, Q. Facilitating Protein Expression with PorTable 5′-UTR Secondary Structures in Bacillus licheniformis. *ACS Synth. Biol.* **2020**, *9*, 1051–1058. [CrossRef] [PubMed]
30. Hofacker, I.L.; Stadler, P.F. Memory efficient folding algorithms for circular RNA secondary structures. *Bioinformatics* **2006**, *22*, 1172–1176. [CrossRef]
31. Codex Alimentarius Commission. *Guideline for the Conduct of Food Safety Assessment of Foods Derived from Recombinant-DNA Plants*; Codex Alimentarius Commission: Rome, Italy, 2003.
32. Robert, X.; Gouet, P. Deciphering key features in protein structures with the new ENDscript server. *Nucleic Acids Res.* **2014**, *42*, W320–W324. [CrossRef] [PubMed]
33. Oliva, M.; Dideberg, O.; Field, M.J. Understanding the acylation mechanisms of active-site serine penicillin-recognizing proteins: A molecular dynamics simulation study. *Proteins* **2003**, *53*, 88–100. [CrossRef] [PubMed]
34. Shin, K.C.; Sim, D.H.; Seo, M.J.; Oh, D.K. Increased Production of Food-Grade d-Tagatose from d-Galactose by Permeabilized and Immobilized Cells of Corynebacterium glutamicum, a GRAS Host, Expressing d-Galactose Isomerase from Geobacillus thermodenitrificans. *J. Agric. Food Chem.* **2016**, *64*, 8146–8153. [CrossRef] [PubMed]